Carbonaceous aerosol source apportionment using the aethalometer model-Evaluation by radiocarbon and levoglucosan analysis at a rural background site in southern Sweden

Johan Martinsson[1,2], Hafiz Abdul Azeem[3], Moa K. Sporre[4], Robert Bergström[5,6], Erik Ahlberg[1,2], Emilie Öström[1,2], Adam Kristensson[1], Erik Swietlicki[1], Kristina Eriksson Stenström[1]

[1]Division of Nuclear Physics, Lund University, Box 118, SE-22100, Lund, Sweden
[2]Centre for Environmental and Climate Research, Lund University, Ecology Building, SE-22362, Lund, Sweden
[3]Centre for Analysis and Synthesis, Department of Chemistry, Lund University, Lund, Box 118, SE-22100, Lund, Sweden
[4]Department of Geosciences, University of Oslo, Postboks 1022, Blindern, 0315, Oslo, Norway
[5]Swedish Meteorological and Hydrological Institute, SE-60176, Norrköping, Sweden
[6]Department of Chemistry, University of Gothenburg, SE-41296, Gothenburg, Sweden

Correspondence to: Johan Martinsson (johan.martinsson@nuclear.lu.se)

Abstract. With the present demand on fast and inexpensive aerosol source apportionment methods, the aethalometer model was evaluated for a full seasonal cycle (June 2014-June 2015) at a rural atmospheric measurement station in southern Sweden by using radiocarbon and levoglucosan measurements. By utilizing differences in absorption of UV and IR, the aethalometer model apportions carbon mass into wood burning (WB) and fossil fuel combustion (FF) aerosol. In this study, a small modification in the model in conjunction with carbon measurements from thermal-optical analysis allowed apportioned non-light absorbing biogenic aerosol to vary in time. The absorption differences between WB and FF can be quantified by the absorption Ångström exponent (AAE). In this study AAE_{WB} was set to 1.81 and AAE_{FF} to 1.0. Our observations show that the AAE was elevated during winter (1.36±0.07) compared to summer (1.12±0.07). Quantified WB aerosol showed good agreement with levoglucosan concentrations, both in terms of correlation (R^2=0.70) and in comparison to reference emission inventories. WB aerosol showed strong seasonal variation with high concentrations during winter (0.65 µg m^{-3}, 56 % of total carbon) and low concentrations during summer (0.07 µg m^{-3}, 6 % of total carbon). FF aerosol showed less seasonal dependence, however black carbon (BC) FF showed clear diurnal patterns corresponding to traffic rush hour peaks. The presumed non-light absorbing biogenic carbonaceous aerosol concentration was high during summer (1.04 µg m^{-3}, 72 % of total carbon) and low during winter (0.13 µg m^{-3}, 8 % of total carbon). Aethalometer model results were further compared to radiocarbon and levoglucosan source apportionment results. The comparison showed good agreement for apportioned mass of WB and biogenic carbonaceous aerosol but discrepancies were found for FF aerosol mass. The aethalometer model overestimated FF aerosol mass by a factor of 1.3 compared to radiocarbon and levoglucosan source apportionment. A performed sensitivity analysis suggests that this discrepancy can be explained by interference of non-light absorbing biogenic carbon during winter. In summary, the aethalometer model offers a cost-effective, yet robust high time resolution source apportionment at rural background stations compared to a radiocarbon and levoglucosan alternative.

1 Introduction

Carbonaceous aerosol, i.e. the fraction of the aerosol containing carbon, is approximately contributing with 25 % to the mass of particulate matter with smaller diameter than 10 μm (PM_{10}) in Europe (Fuzzi et al., 2015) and is presently estimated to be one of the most important climate forcers (IPCC, 2013). However, the magnitude of the carbonaceous aerosol impact on climate is still associated with significant uncertainty (IPCC, 2013). The carbonaceous aerosol originates mainly from three sources; wood burning, fossil fuel combustion and biogenic emissions. Black carbon (BC) or soot is formed from incomplete combustion of fossil fuels and biofuels. BC has a graphitic carbon structure and is known to efficiently absorb incoming solar radiation (Bond et al., 2013). This absorption leads to molecular vibration and rotation which causes emission of longwave radiation, heating the atmosphere. On the other hand, the organic aerosol (OA) is known to mainly scatter incoming sunlight, thereby cooling the climate. Recently, the strongly ultraviolet-absorbing brown carbon (BrC) has gained interest in the scientific community (Laskin et al., 2015;Martinsson et al., 2015;Saleh et al., 2013;Saleh et al., 2014). BrC is emitted in large quantities from wood burning and has been proposed to affect lower tropospheric photochemistry by reducing ultraviolet (UV) radiation (Jacobson, 1999). Although BrC is a much less effective light absorber than BC, deposition of BrC on bright surfaces such as snow or ice may cause significant changes in albedo (Doherty et al., 2010).

Carbonaceous aerosols have also been linked to serious health effects, mainly through inhalation (Grahame et al., 2014;Laden et al., 2006;Pope and Dockery, 2006). Carbonaceous aerosols derived from wood burning have been shown to be hazardous to humans (Barregard et al., 2006;Eriksson et al., 2014;Jalava et al., 2010;Naeher et al., 2007;Sehlstedt et al., 2010;Unosson et al., 2013). Additionally, diesel and gasoline vehicles emit large quantities of BC and associated compounds (e.g. polycyclic aromatic hydrocarbons, PAH) which have been suggested as one of the most health-damaging particle types (Benbrahim-Tallaa et al., 2012;Hoek et al., 2002;Salvi et al., 1999).

One of the re-emerging air pollutants in Europe is particles from residential wood burning (van der Gon et al., 2015). Wood burning is increasing with approximately 3.5 % per year in Europe due to its potential CO_2-neutral effect on climate, while the fossil energy consumption is decreasing by 2 % per year (EEA, 2015). Particle emissions from residential wood burning are usually elevated during winter. It has been estimated that 45-65 % of the total ambient carbonaceous aerosol mass (TC) in Europe is associated with wood burning during this period of the year (Gilardoni et al., 2011;Szidat et al., 2006). Due to the severe climate and health effects from different particle sources, and the importance of wood burning in particular, it is crucial to develop and evaluate source apportionment methods of the carbonaceous aerosols. An accurate source apportionment enables justified mitigation of particle emissions that affect health and climate, as well as a possibility to evaluate emission inventories and chemical transport models.

Levoglucosan is an anhydrosugar formed during pyrolysis of cellulose at temperatures above 300 °C (Simoneit, 2002). Due to its specificity for cellulose combustion, it has been widely used as a molecular tracer for wood burning in source apportionment studies (Gelencser et al., 2007;Genberg et al., 2011;Yttri et al., 2011a;Yttri et al., 2011b). However, there are some drawbacks of using levoglucosan for this purpose. Several studies have shown that levoglucosan may not be stable in

the troposphere, it may react with OH both in the gas-phase (Hennigan et al., 2010;May et al., 2012) and aqueous phase (Hoffmann et al., 2010;Zhao et al., 2014) leading to relatively short estimated atmospheric life-times of 1-5 days, depending on the season and atmospheric conditions. The importance of the degradation of levoglucosan in the ambient atmospheric aerosol is still not clarified (Yttri et al., 2015). Also, the relative levoglucosan contribution to the carbonaceous aerosol mass

5   is dependent on combustion conditions (Hedberg and Johansson, 2006). Levoglucosan is most commonly measured on aerosol-laden filters. Filter sampling is generally associated with low time resolution which makes it difficult to study rapid variations of this source marker.

More recently, the aethalometer model (Sandradewi et al., 2008a), employing multi-wavelength light absorbing measurement techniques with high time resolution, has been used for a number source apportionment studies (Favez et al.,

10   2009;Favez et al., 2010;Herich et al., 2011;Sandradewi et al., 2008a), as an alternative to the methods based on chemical analysis of filter samples. This method relies on the assumption that particles generated from wood burning are relatively more light-absorbing in the UV than infrared (IR) compared to particles from traffic and other fossil fuel combustion (Kirchstetter et al., 2004). The difference in light absorption can be quantified using the absorption Ångström exponent (AAE) which is a measure of the spectral absorption dependence (Kirchstetter et al., 2004). Wood burning emissions are

15   assumed to have an AAE between 1.5-2.5 while traffic and fossil fuel combustion derived particles exhibits an AAE around 1.0 (Kirchstetter et al., 2004). Despite the great benefits the light-absorption based source apportionment can offer, with its high time resolution and low costs, the relations between the highly source specific levoglucosan and light absorption measurement derived aethalometer model parameters have so far not been thoroughly investigated. Some studies have found good correlation between levoglucosan and AAE, or calculated BC from wood burning (BC$_{WB}$), using the aethalometer

20   model (Fuller et al., 2014;Herich et al., 2011;Lack et al., 2013). On the other hand, recently published studies claim that the aerosol spectral dependence is more affected by combustion conditions than the type of fuel being combusted (Garg et al., 2016;Martinsson et al., 2015). Garg et al. (2016) found that the gaseous tracer for biomass burning, acetonitrile, correlated well with AAE during smoldering combustion but poorly during flaming combustion, and further that AAE varied greatly throughout combustion of the same fuel type. Calvo et al. (2015) measured levoglucosan in a wood stove with controlled

25   combustion and a traditional fireplace; they found elevated concentrations of levoglucosan during the fuel addition followed by a rapid decrease in concentration in the flaming phase. Hence, it is possible that observed correlations between AAE and levoglucosan may only be valid for the smoldering combustion, which may limit the use of both levoglucosan and AAE as universal tracers of biomass burning.

The aethalometer model has so far mainly been applied during winter in highly polluted urban environments (Favez et al.,

30   2009;Favez et al., 2010;Fuller et al., 2014;Harrison et al., 2013;Sandradewi et al., 2008a). There is thus a lack of knowledge regarding the performance of the aethalometer model during summer, and in less polluted rural environments. For instance, it is not known how the aethalometer model will cope with the usually dominating and presumably non-light absorbing biogenic secondary organic aerosol (SOA) during summer.

This study was initiated with the aim to compare a light-absorption source apportionment technique, the aethalometer model (Sandradewi et al., 2008a), to traditional filter-based chemical and physical analysis source apportionment using radiocarbon and levoglucosan measurements for a whole year at a rural measurement station in southern Sweden.

2 Methods

2.1 Measurement site and sampling

Sampling of atmospheric aerosols was conducted at the aerosols, clouds and trace gases research infrastructure (ACTRIS) and European monitoring and evaluation programme (EMEP) rural background station Vavihill, located in southern Sweden (56°01' N, 13°09' E, 172 meters above sea level). The surrounding landscape consists of coniferous and deciduous forests, farmland and pastures. The measurement station is placed on a pasture that is visited by grazing cattle during spring, summer and fall. The closest large cities are Helsingborg, Malmö and Copenhagen which are located at distances of 20, 50 and 65 km in the west to southwest direction, respectively. Aerosols were sampled with a PM_{10}-inlet on pre-heated (900 °C for 4 h in air) 47 mm quartz filters (Pallflex 2500QAT-UP) using a sampling time of 72 h at a flow rate of 38 liters per minute (lpm) with an automatic Leckel SEQ47/50 sampler. The sampling line consisted of active carbon denuders followed by two quartz filters in series (i.e. front and back filters) with the purpose of correcting for any sampling artefacts caused by volatile organic compounds (VOCs). The installed denuders have shown an efficiency of 90-95 % in a denuder test conducted at Vavihill 2008-2009 (Genberg et al., 2011). However, sampling through active carbon denuders may change the gas-particle equilibrium at the filter, leading to evaporation of semi-volatile compounds from the filter. Genberg et al. (2011) observed that field blanks had similar carbon concentration as the back filters, and consequently concluded that this negative artefact was small. Hence, no correction was considered in the present study. After sampling, filters were put in petri dishes, wrapped in aluminium foil and stored in a freezer at -18 °C until analysis. The total measurement period lasted from June 2014 until June 2015 and included in total 123 filter samples. The measurement period was divided into seasons with 3 months intervals, summer=June-August, fall=September-November, winter=December-February and spring=March-May.

2.2 OC/EC analysis

Elemental carbon (EC), organic carbon (OC) and total carbon (TC) were measured through thermal-optical analysis (TOA) with a DRI Carbon analyzer (Model 2001). The EUSAAR_2 analytic protocol was used for the analysis (Cavalli et al., 2010). In short, OC from a 0.5 cm^2 filter punch is evolved in four different temperature steps in an inert helium atmosphere at a maximum temperature of 570 °C. A 633 nm He/Ne-laser is irradiating the filter and the light transmission through the filter is measured during the increase of temperature. When the measured light transmission reaches its initial base-line value the remaining carbon is considered to be EC. EC is evolved in an oxidizing atmosphere (2 % O_2) during high temperatures (500-850 °C). All carbon is oxidized and evolved from the filter as CO_2, which is further converted to methane and finally quantified with a flame ionization detector (FID). TC is the sum of OC and EC. Cavalli et al. (2016) estimated the combined

random uncertainties from inter-laboratory comparisons between 2008-2011 to be 17 % relative standard deviations (RSD) for Vavihill TC measurements.

2.3 Light absorption measurements and the aethalometer model

Aerosol light absorption was measured with an aethalometer (AE33, Magee Scientific) (Drinovec et al., 2015). The aethalometer utilizes an airflow through a filter where particles are deposited. The filter deposition spot is irradiated with seven LEDs of different wavelengths (370, 470, 520, 590, 660, 880, 950 nm) and the attenuation is calculated per unit of time. In this campaign the aethalometer was operating with a flow of 5 liters per minute through a PM_{10} inlet at a time resolution of 1 minute. Two main measurement artefacts are associated with filter-based light absorption techniques; the shadowing effect and the filter matrix scattering effect (Weingartner et al., 2003). The AE33 aethalometer handles these artefacts in two ways: attenuation enhancement due to filter matrix scattering is compensated by a factor 1.57, and the shadowing effect is treated by measuring the attenuation at two filter deposition spots with different depositions rates (Drinovec et al., 2015).

The output data of the aethalometer are absorption coefficients, $b_{abs}(\lambda)$, in the units of m^{-1}. $b_{abs}(\lambda)$ can be converted into BC mass concentration units (g m^{-3}) by division of the mass absorption coefficient (MAC), $\sigma_{abs}(\lambda)$ (m^2 g^{-1}) according to Eq (1):

$$BC(\lambda) = \frac{b_{abs}(\lambda)}{\sigma_{abs}(\lambda)} \tag{1}$$

In the aethalometer model (Sandradewi et al., 2008a), the entire aerosol light absorption is assumed to come from fossil fuel combustion aerosol (FF) or wood burning aerosol (WB):

$$b_{abs}(\lambda) = b_{absFF}(\lambda) + b_{absWB}(\lambda) \tag{2}$$

$$\frac{b_{absFF}(370nm)}{b_{absFF}(950nm)} = \left(\frac{370}{950}\right)^{-AAE_{FF}} \tag{3}$$

$$\frac{b_{absWB}(370nm)}{b_{absWB}(950nm)} = \left(\frac{370}{950}\right)^{-AAE_{WB}} \tag{4}$$

By combining Eq. (2-4), it is now possible to calculate the light absorption that is caused by WB and FF in 370 and 950 nm (Mohr et al., 2013;Zotter et al., 2016), respectively:

$$b_{absFF}(950nm) = \frac{b_{abs(370nm)} - b_{abs(950nm)} \cdot \left(\frac{370}{950}\right)^{-AAE_{WB}}}{\left(\frac{370}{950}\right)^{-AAE_{FF}} - \left(\frac{370}{950}\right)^{-AAE_{WB}}} \tag{5}$$

$$b_{absWB}(370nm) = \frac{b_{abs(370nm)} - \left(\frac{370}{950}\right)^{-AAE_{FF}} \cdot b_{abs(950nm)}}{1 - \frac{\left(\frac{370}{950}\right)^{-AAE_{FF}}}{\left(\frac{370}{950}\right)^{-AAE_{WB}}}} \tag{6}$$

In Eq. (3-6) the AAE is the source specific spectral dependence. In the aethalometer model, the selection of source specific AAEs (AAE_{FF} and AAE_{WB}) are crucial for accurate source contribution estimation. Traditionally, is has been assumed that pure black carbon is dominating fossil fuel combustion emission, leading to an AAE_{FF}=1. Wood burning emissions have previously been assumed to have an AAE around 2 (Kirchstetter et al., 2004). However, recent studies have shown that it is

the combustion conditions rather than the fuel itself that determines the organic content in the aerosol, and consequently the AAE (Garg et al., 2016;Martinsson et al., 2015). Martinsson et al. (2015) found that flaming combustion in a modern conventional wood stove emitted aerosol with highly agglomerated soot structure and an AAE of 1.3. Garg et al. (2016) determined the combustion efficiency by analysing emission gas data and reached similar conclusions. We estimated AAE_{FF}

5 and AAE_{WB} based on literature data (Table 1). From Table 1 a mean $AAE_{FF}=1.0$ (SD=0.1) and mean $AAE_{WB}=1.81$ (SD=0.52) was chosen in this study. The value of $AAE_{WB}=1.81$ is close to the values chosen by Massabo et al. (2015) and Sandradewi et al. (2008a), i.e. 1.81 and 1.86, respectively.

By using Eq. (5-6) it is possible to calculate the light absorption due to FF ($b_{absFF}(\lambda)$) or WB ($b_{absWB}(\lambda)$). These light absorption coefficients can then be divided with the site specific MAC (Table 2) in order to calculate the BC mass

10 concentration from each source (Eq. 7-8):

$$BC_{FF} = \frac{b_{absFF}(950nm)}{\sigma_{abs}(950nm)} \tag{7}$$

$$BC_{WB} = \frac{b_{absWB}(370nm)}{\sigma_{abs}(370nm)} \tag{8}$$

$\sigma_{abs}(\lambda)$ is in this case the site-specific mass absorption coefficients for the respective wavelengths which can be found in Table 2. Site specific $\sigma_{abs}(\lambda)$ was determined by linear regression of $b_{abs}(\lambda)$ against elemental carbon (EC) concentration in

15 PM_{10}. However, it should be noted that OC also may absorb light, which can result in an overestimated site specific $\sigma_{abs}(\lambda)$ by using the regression between $b_{abs}(\lambda)$ and EC. However, EC is believed to be a much stronger light absorber than light absorbing OC (Bond and Bergstrom, 2006;Laskin et al., 2015), therefore this overestimation is believed to be small. It is also possible to calculate the carbonaceous aerosol mass (CM, i.e. the sum of primary and secondary aerosol) from FF and WB, together with non-light absorbing secondary aerosol. The latter is presumably mostly derived from biogenic sources, hence

20 the acronym CM_{Bio}:

$$TC = CM_{FF} + CM_{WB} + CM_{Bio} = C_1 \cdot b_{absFF}(950nm) + C_2 \cdot b_{absWB}(370nm) + CM_{Bio} \tag{9}$$

In Eq. (9), C_1 and C_2 are the slopes from the linear regression of measured total carbonaceous matter (TC) and the light absorption due to FF ($b_{absFF}(950nm)$) and WB ($b_{absWB}(370nm)$), respectively. Previous work has set CM_{Bio} as the intercept when solving the multilinear equation, however this is highly unrealistic since biogenic primary and secondary aerosol formation is seasonal dependent and should vary accordingly (Guenther et al., 1995). We propose an alternative method

25 where CM_{Bio} is allowed to vary outside the suggested regressions (Eq. 10-12). If Eq. (9) is rewritten, a linear regression can be used in order to calculate C_1 and C_2:

$$\frac{TC}{b_{absWB}(370nm)} = C_1 \cdot \frac{b_{absFF}(950nm)}{b_{absWB}(370nm)} + C_2 + \frac{CM_{Bio}}{b_{absWB}(370nm)} \tag{10}$$

$$\frac{TC}{b_{absFF}(950nm)} = C_2 \cdot \frac{b_{absWB}(370nm)}{b_{absFF}(950nm)} + C_1 + \frac{CM_{Bio}}{b_{absFF}(950nm)} \tag{11}$$

30 For Eq. (10), C_1 can be calculated as the slope of the regression line by setting $TC/b_{absWB}(370nm)$ as the dependent variable and $b_{absFF}(950nm)/b_{absWB}(370nm)$ as the independent. A similar approach can be applied to Eq. (11) to calculate C_2. By selecting only winter data for calculation of C_1 and C_2 the interference of CM_{Bio} is minimized and the division of CM_{Bio} by

one of the light absorption parameters is forcing CM_{Bio} towards zero. Hence, the intercept of the linear regression line should be close to C_2 when calculating the slope as C_1 in Eq. 10, and vice versa for Eq. 11. The linear fits used to derive C_1 and C_2 contained one suspected outlier each. These outliers were confirmed by Grubbs test (Grubbs, 1950) for both dependent and independent variables with 95% confidence and hence removed. The linear fits without outliers are displayed in Fig. S1 and

5 S2. Finally, CM_{Bio} is allowed to vary outside the linear regressions:

$$CM_{Bio} = TC - CM_{FF} - CM_{WB} \qquad (12)$$

Since CM_{Bio} is assumed to be the residual carbonaceous matter, i.e. the carbonaceous matter that does not absorb light, this parameter may have a negative value during winter when the sum of CM_{FF} and CM_{WB} exceeds TC.

C_1 was calculated to be 214 467 µg m^{-2} with an intercept of 133 794. C_2 was estimated to 113 881 µg m^{-2} with an intercept of

10 273 603. Hence, C_1 (from Eq. 10) was deviating 22 % from the intercept in the calculation of C_2 (Eq. 11), while C_2 (from Eq. 11) was deviating 15 % from the intercept in the calculation of C_1 (Eq. 10).

Herich et al. (2011) found high standard errors in their modelled C_1 and C_2 parameters ($\pm$ 30 %). This was the main reason for Herich et al. (2011) to exclude the CM-approach and proceed with the BC approach presented in Eq. (7-8). In comparison to Herich et al. (2011), we found similar standard error for C_1 (31 %) but lower for C_2 (18 %). We have therefore

15 chosen to proceed with the CM-approach.

2.4 Levoglucosan analysis

1,6-Anhydro-beta-D-glucose (levoglucosan) analysis was performed using the method of Wu et al. (2008) with some modifications. Levoglucosan was purchased from Sigma Aldrich (St. Louise, USA). Hexane from Scharlau (Spain), 1-phenydodecane, 97 % from Acros Organics (Geel, Belgium) and N,O-bis(trimethylsilyl)trifluoroacetamide (BSTFA)

20 containing 1 % trimethylsilyl chloride (TMCl) was purchased from Sigma (St. Louise, USA). Filter punches were divided into small pieces using a surgical blade and placed in a 50 ml conical flask. Extraction was carried out by sonication using three aliquots of 15 ml, 10 ml and 10 ml of dichloromethane and methanol (1:3) for 45 minutes, 30 minutes and 15 minutes respectively. Extract from each step was filtered and pooled together in a 50 ml beaker using a 0.45 µm polypropylene membrane syringe filter. The total extract was concentrated to dryness under a gentle stream of nitrogen at 60 °C. The final

25 volume of the extract was made up to 1 ml with dichloromethane.

50 µl of each extract was placed in gas chromatography (GC) vials with 300 µl glass inserts and evaporated to dryness under a gentle stream of nitrogen at 60 °C. 15 µl of 1-phenydodecane (97 % Acros Organics, internal standard) solution prepared in hexane (1 µg ml^{-1}) and 10 µl of N,O-bis(trimethylsilyl)trifluoroacetamide (BSTFA) containing 1 % trimethylsilyl chloride (TMCl) were added to the vials (Sigma-Aldrich). The vials were sealed using screw caps with Teflon septa. Samples were

30 derivatized in an oven at 80 °C for 1 h. Solvent blanks and calibration curve were run for each batch of eight samples. Samples were analyzed immediately after derivatization.

An Agilent 6890 series GC with 5973 MS (Agilent Technologies, Palo Alto, USA) was used for the analysis. An Agilent HP-5ms column (30 m x 0.25 mm x 0.25 µm film thickness) was used. Injection volume was 2 µl, splitless, with injector

temperature of 280 °C. The temperature program was as follows; initial temperature 60 °C for 3 minutes then the temperature was raised to 190 °C at a rate of 10 °C min^{-1} and then it was finally raised to 300 °C at a rate of 30 °C min^{-1}. Transfer line, ion source and quadruple temperatures were 280 °C, 250 °C and 180 °C, respectively. The MS was operated in electron ionization mode. Scan mode was used to identify levoglucosan (99 % pure, Sigma-Aldrich) and 1-phenyldodecane

5   with m/z 217 and 246 respectively. The exact masses used for calibration curves and aerosol samples were determined by SIM mode as m/z 217.3 and 246.3, respectively. The measurement uncertainty in SD of the GC-MS measurements was estimated to be ±1 % of the levoglucosan peak areas.

2.5 ^{14}C analysis

The ^{14}C/^{12}C ratio in the sampled particles was measured with accelerator mass spectrometry (AMS) (Hellborg and Skog,

10   2008) by using the 250 kV single-stage AMS at Lund University (Skog, 2007;Skog et al., 2010). Prior to the analysis, the carbon in the particle filter sample was transformed to graphite according to the procedure described in Genberg et al. (2010). In brief, a filter sample corresponding to approximately 50 µg carbon was mixed with CuO and combusted in a vacuum. Evolved CO_2 was purified cryogenically, mixed with H_2 and heated to 600 °C in the presence of an iron catalyst. In the latter reaction the CO_2 was reduced into graphite. The results are presented as fraction modern carbon, F^{14}C (Reimer et

15   al., 2004). A F^{14}C value of 1 represents the 1950 concentration of ^{14}C excluding human influences. The true atmospheric ^{14}C content has however been altered due to two effects, known as the bomb effect (Rafter and Fergusson, 1957) and the Suess effect (Suess, 1955). The bomb effect, which is referring to atmospheric testing of thermonuclear weapons in the 1940-1960s, has had a positive effect on the F^{14}C values, due to neutron-induced reactions forming ^{14}C. The Suess effect is the result of emission of CO_2 from anthropogenic fossil fuel combustion, leading to the ongoing increase of the atmospheric CO_2

20   concentration. Since fossil fuels are ^{14}C-free, the Suess effect generates decreased F^{14}C values of atmospheric carbon (Baxter and Walton, 1970). Estimated measurement uncertainties expressed as SD, are typically ±1 % of measurement values.

Prior to the F^{14}C measurements, 104 out of 123 filter samples were pooled with a neighbouring sample due to limited amount of filter material. In the pooled samples, filter material corresponding to 25 µg C were punched out from each of the two filter samples, resulting in the desirable mass of 50 µg C. Two pooled samples (19th-25th December 2014 and 17th-23rd

25   February 2015) were omitted due to failure in the graphitization process and consequently lack of filter material.

Evaluation of the aethalometer model results was performed using mainly F^{14}C data and the source apportionment approach by Bonvalot et al. (2016). The ambient carbonaceous aerosol can be assumed to be composed of one fossil and one non-fossil fraction. Determination of the non-fossil fraction (f_{NF}) is performed by normalizing the measured F^{14}C (F^{14}C$_S$) by a non-fossil reference value (F^{14}C$_{NF,ref}$):

30   $$f_{NF} = \frac{F^{14}C_S}{F^{14}C_{NF,ref}}$$ (13)

A previous source apportionment study at Vavihill suggests that winter samples are highly influenced by wood burning but low levels of other modern carbon sources, i.e. biogenic primary and secondary aerosol (Genberg et al., 2011). Biomass used

for wood burning has usually had a growth period of decades, implying that the integrated average $F^{14}C$ for wood burning is higher than the atmospheric $F^{14}C$ at the time of sampling. As in previous studies, we also assume that the biomass used in wood burning has an average $F^{14}C_{WB}$ of 1.10 (Szidat et al., 2006;Bonvalot et al., 2016). Hence, we use $F^{14}C_{NF,ref}$=1.10 during winter.

5   Summer carbonaceous aerosol mass at Vavihill has been found to be dominated by biogenic primary and secondary organic aerosol (Genberg et al., 2011;Yttri et al., 2011a). Hence, the summer time carbonaceous aerosol should have a $F^{14}C$ close to the atmospheric value at the sampling time, i.e. $F^{14}C_{Bio}$=1.04. Thus, summer time $F^{14}C_{NF,ref}$ was set to 1.04. Spring and fall are characterized by highly mixed sources of modern carbon. It can be expected that both wood burning and biogenic emissions contribute significantly to the carbonaceous mass during these seasons. We therefore chose the mean of winter and

10   summer $F^{14}C_{NF,ref}$ to represent the spring and fall samples, i.e. 1.07. The total carbon can be assumed to be derived from three possible sources:

$$TC = TC_{NF} + TC_{FF} = TC_{WB} + TC_{Bio} + TC_{FF} \qquad (14)$$

In Eq (14), sample TC is divided into non-fossil (NF) and fossil fractions (FF). NF can be further subdivided into wood burning (WB) and biogenic carbon (Bio). From Eq. (14) it is now possible to set up the ^{14}C mass balance equation:

15   $$TC \cdot F^{14}C_S = TC_{WB} \cdot F^{14}C_{WB} + TC_{Bio} \cdot F^{14}C_{Bio} + TC_{FF} \cdot F^{14}C_{FF} \qquad (15)$$

In Eq. (15) $F^{14}C_S$ is the sample $F^{14}C$. $F^{14}C_{WB}$, $F^{14}C_{Bio}$ and $F^{14}C_{FF}$ are the reference $F^{14}C$ value for each of the respective sources. Since $F^{14}C_{FF}$ is equal to zero, this gives:

$$TC \cdot F^{14}C_S = TC_{WB} \cdot F^{14}C_{WB} + TC_{Bio} \cdot F^{14}C_{Bio} \qquad (16)$$

TC non-fossil (TC_{NF}) can be calculated by Eq. (17):

20   $$TC_{NF} = TC \cdot f_{NF} \qquad (17)$$

Total carbon from wood burning (TC_{WB}) can then be calculated by Eq. (18):

$$TC_{WB} = a \cdot [levoglucosan] \qquad (18)$$

Here, a is the slope from the linear fit between TC_{NF} and levoglucosan for winter samples (Fig. S3), [levoglucosan] is the sample levoglucosan concentration. Only winter samples are used and the linear fit is forced through origin with the purpose

25   of minimizing the effect of biogenic carbon on TC_{NF}. Hence, we assume that all non-fossil carbon is derived from wood burning during winter. However, it should be noted that combustion of fossil lignite (i.e. brown coal), can emit large quantities of levoglucosan and be confused with wood combustion (Fabbri et al., 2008). It is now possible to calculate the total carbon from biogenic sources:

$$TC_{Bio} = \frac{F^{14}C_S \cdot TC - TC_{WB} \cdot F^{14}C_{WB}}{F^{14}C_{Bio}} \qquad (19)$$

30   In Eq. (19), $F^{14}C_S$ is the sample $F^{14}C$, $F^{14}C_{WB}$=1.10 and $F^{14}C_{Bio}$=1.04 (Bonvalot et al., 2016). Finally, it is possible to derive TC_{FF}:

$$TC_{FF} = TC - TC_{WB} - TC_{Bio} \qquad (20)$$

2.6 HYSPLIT

The Hybrid Single Particle Lagrangian Integrated Trajectory Model (HYSPLIT) (Draxier and Hess, 1998;Stein et al., 2015) was used to study the history of the air mass carrying the particles sampled on the filters and measured by the aethalometer. Gridded meteorological data from the Centre of Environmental Predictions (NCEP) Global Data Assimilation System (GDAS) were used as input to trajectory model. Back-trajectories were calculated at an hourly frequency 120 h backward in time and the trajectories started 100 m above ground at the Vavihill measurement site. For each filter sample, 72 trajectories were used since the sampling time was 72 h. Four regions of origin (Table 3) were defined and for each sample it was investigated how much time the air-mass had spent over each of the regions of origin. Also, the accumulated precipitation along each trajectory during the last 24 h before arrival at Vavihill was used to evaluate the effect of precipitation on aerosol particle concentration. For each sample, the accumulated precipitation along each of the 72 the trajectories were summarized.

2.7 Auxiliary measurements

NO_X was continuously monitored with a time resolution of 1 h with a CLD 700 AL chemiluminescence analyzer (Eco Physics, Duernten, Switzerland). The detection limit was 1 ppb. Mass concentration of PM_{10} was monitored with a tapered element oscillating microbalance (TEOM, 8500 FDMS, ThermoFisher Scientific). The time resolution was 1 h and detection limit 0.1 µg m^{-3}.

3 Results and discussion

3.1 Variations and features in carbon concentrations

Carbonaceous aerosol constitutes on average 13 % of the total PM_{10} during the measurement period. Figure 1a-b displays the temporal variation of particulate carbon throughout the measurement period. OC is elevated during summer (mean=1.29 µg m^{-3}) and fall (mean=1.86 µg m^{-3}) and then decrease during winter (mean=0.96 µg m^{-3}) and spring (mean=1.19 µg m^{-3}). EC peaked during fall (mean=0.32 µg m^{-3}) while the concentrations during winter (mean=0.19 µg m^{-3}), spring (mean=0.21 µg m^{-3}), and summer (mean=0.14 µg m^{-3}) were significantly lower ($p < 0.05$, Fig. 1b).

A discrepancy in winter concentrations of carbonaceous compounds was found between this study (2014-2015) and a previous Vavihill source apportionment study (2008-2009). Genberg et al. (2011) found elevated concentrations of OC during winter (2.19 µg m^{-3}, $p < 0.1$) and approximately twice the amount of EC during winter compared to summer (0.30 µg m^{-3} vs. 0.14 µg m^{-3}, $p < 0.001$). EC is typically elevated during the cold period of the year, when residents burn wood for heating. In the present study we found no significant differences in OC or EC between summer and winter. Figure 1a reveals a decrease in carbonaceous aerosol mass concentration during winter, from the beginning of December 2014 to mid-February 2015. In fact, by comparing the measurement campaign TC during the winter 2014-2015 with the average TC during earlier winters we found that the TC concentration during the winter 2014-2015 was 35 % lower than the average

winter of 2008-2013 (p=0.024, Fig. S4). By using HYSPLIT we find that the incoming air masses to Vavihill during the winter of this measurement campaign were influenced by approximately 45 % more precipitation than the average winter of 2000-2013 (p=0.002, Fig. S5). Furthermore, we found a weak but significant negative relationship between precipitation and TC (R^2=0.1; p<0.05). Wet deposition losses are thus likely to be at least a partial explanation of lower winter-time concentrations of carbonaceous aerosol in this study.

3.2 Variations in light absorption measurements and aethalometer model derived parameters

Figure 2 shows the AAE throughout the whole measurement campaign (June 2014–June 2015). In general, there was a strong negative relationship between AAE and ambient temperature (R^2=0.74; p<0.001). During summer the AAE remains low in the range of 1.0-1.2 (mean=1.12; standard deviation=0.07). An increase in AAE follows during the fall (mean=1.23; SD=0.1) and stays at 1.2-1.5 (mean=1.36; SD=0.07) throughout the winter period. In the spring, the AAE remains high (mean=1.31; SD=0.09), but is decreasing towards 1.1-1.2 at the end of the season. There is a significant difference in AAE between all seasons (p<0.01), except between winter and spring (p=0.055). The observed seasonal pattern is in accordance with earlier studies by Sandradewi et al. (2008b) and Herich et al. (2011) who found elevated AAE of 1.3-1.6 during winter and a decreased AAE of around 1.0 during summer.

Elevated AAE during the cold period of the year is most likely caused by increased use of wood burning for residential heating, this has been confirmed in several studies (Genberg et al., 2011;Herich et al., 2011;Sandradewi et al., 2008b). Since the measured aerosol light absorption most likely is a mixture of fossil and wood burning the selection of AAEs for the aethalometer model calculations are supported by the observed seasonal pattern, i.e. the observed AAE vary between AAE_{FF} and AAE_{WB}.

Figure 3 shows the diurnal variation of AAE (370-950 nm), BC_{FF}, BC_{WB} and NO_X between summer and winter and between weekdays and weekends. There is a minimum in AAE at 7-10 AM (local time, Fig. 3a-b), this coincide with morning traffic rush hours. Sandradewi et al. (2008b) found similar results during winter with a minimum in AAE around 8 AM. This result is confirmed by data presented in Fig. 3d, which shows the calculated BC_{FF} (950nm) from the aethalometer model. It is clear that there is a peak at 8-10 AM and at 5-7 PM in the BC_{FF} emissions. This pattern is validated by NO_X concentrations showing similar diurnal pattern as BC_{FF} (Fig. 3g-h), although the diurnal variation is stronger for the NO_X concentrations. Rissler et al. (2014) found similar peaks in NO_X and BC from a busy road in Copenhagen. A major source of NO_X is vehicle combustion engines and NO_X can thus be expected to correlate with BC_{FF}. Due to the rural location of Vavihill measurement station, it may take 2-3 h for the traffic emissions to reach the station if they originate from the major cities in the region, this can explain why the NO_X (and BC_{FF}) peaks occur somewhat later at Vavihill than expected traffic rush hours. Studying the long-term pattern between BC_{FF} and NO_X, there is a weak but significant correlation throughout the whole measurement campaign (R^2=0.09; p<0.001). However, since NO_X is efficiently oxidized by OH-radicals and ozone during periods with high UV-radiation it is more suitable to compare these on a seasonal basis. Significant but very weak correlations between

BC_{FF} and NO_X were found during fall ($R^2=0.07$; $p=0.021$), winter ($R^2=0.2$; $p<0.001$), spring ($R^2=0.41$; $p<0.001$) and summer ($R^2=0.09$; $p=0.009$). The CM_{FF} parameter shows similar pattern as BC_{FF} to NO_X.

The BC_{WB} concentration has a different diurnal pattern than BC_{FF}. In general, there is a peak in the BC_{WB} concentration from 7 PM to 3 AM (Fig. 3f), which indicates that most residents warm their houses by wood burning during the evenings and nights. Previous studies have found a similar diurnal pattern for wood burning derived emissions (Favez et al., 2010;Harrison et al., 2012;Harrison et al., 2013;Kristensson et al., 2013;Wang et al., 2011).

NO_X is not thought to be emitted in large quantities from wood burning, still NO_X and CM_{WB} concentrations are correlated during the whole measurement period ($R^2=0.31$; $p<0.01$). This can be explained by the fact that both parameters are strongly seasonal dependent, but for different reasons. NO_X is mainly emitted from traffic, a source with usually low seasonal dependence. However, since NO_X is susceptible to photo-oxidation, its lifetime will be decreased during summer and increased during winter. Hence, observed NO_X concentrations may be lower during summer and elevated during winter. CM_{WB} concentrations will be elevated during winter when residents heat their homes and mostly absent during summer. Hence, the correlation is strong but causality is most likely absent between them.

The seasonal patterns of other aethalometer model derived parameters are presented in Table 4 and Fig. 4. It is clear that the wood burning derived carbonaceous aerosol, CM_{WB}, follows a seasonal cycle with high concentrations during fall (mean=0.49 µg m^{-3}), winter (mean=0.65 µg m^{-3}) and spring (mean=0.51 µg m^{-3}), and low levels during summer (mean=0.07 µg m^{-3}). The CM_{WB} peaks with 5 % contribution to PM_{10} during winter, in summer the CM_{WB} contribution is low (0.6 %). The CM_{WB} contribution to TC peaks in winter with 56 % and is reduced to 6 % during summer. Hence, it is likely that the largest part of wood burning is conducted with the purpose of residential heating, as in contrast to decorative burning which can be expected independently of outdoor temperature.

The fossil fuel derived parameter, CM_{FF}, shows a less distinct seasonal pattern than CM_{WB}, most probably because the main source, traffic, has a much smaller seasonal variation than wood burning. CM_{FF} contributed 2-4 % to PM_{10} during the year (21-35 % contribution to TC) with a maximum during spring and a minimum during summer. Finally, the biogenic aerosol carbon concentrations are substantial during summer (9 % of PM_{10}; 72 % of TC) and low during winter (0.9 % of PM_{10}; 8 % of TC).

3.3 Comparison: Levoglucosan to aethalometer model

Levoglucosan concentrations displayed an annual variation with elevated concentrations during the cold period of the year (Fig. S6). Mean concentrations during fall, winter and spring were 0.061 (SD±0.082), 0.086 (SD±0.073) and 0.063 (SD±0.115) µg m^{-3}, respectively. The summertime mean levoglucosan concentration was 0.014 (SD±0.0142) µg m^{-3}. There was a significant difference between winter and summer (p=0.03). Measured concentration levels and seasonal patterns were similar to those found by Genberg et al. (2011) at the same measurement site. The aethalometer model derived carbonaceous matter from wood burning, CM_{WB}, correlated well with levoglucosan (Fig. 5, $R^2=0.7$; $p<0.001$). The correlation was strongest during winter ($R^2=0.82$) and spring ($R^2=0.81$) and lower during fall ($R^2=0.37$) and summer ($R^2=0.30$). Mean

measured levoglucosan per unit of BC_{WB} was estimated to 0.64 (standard deviation=0.73). Previous wood stove measurements report mean levoglucosan to EC ratio of 0.82 (Iinuma et al., 2007;Schmidl et al., 2008). Thus, the estimated ratios presented in this study are in line with emission inventories from wood stoves. The measured ratios in comparison to references imply that the atmospheric decomposition of levoglucosan is in general slow, at least during the cold seasons.

5   Another possibility is that the wood burning sources are located fairly close to the sampling site.

Further, CM_{FF} is also correlated with levoglucosan throughout the whole year (R^2=0.39; p<0.001). This finding is in contrast to Herich et al. (2011) who found no correlation between BC_{FF} and levoglucosan in the alpine regions of Switzerland. One explanation might be inaccurate apportionment where the wood burning aerosol exhibits an AAE close to 1, and thus being apportioned as fossil fuel aerosol. This hypothesis is supported by the study of Martinsson et al. (2015), but whether this

10   phenomenon would be more common and pronounced in Swiss alpine regions in comparison to southern Sweden is unknown.

3.4 Aethalometer model evaluation by radiocarbon and levoglucosan source apportionment

We used $F^{14}C$ and levoglucosan data (Fig. S6-7) applied to the method proposed by Bonvalot et al. (2016) to evaluate the aethalometer model parameters. In Eq. (18), a was set to 8.32 based on results from linear regression between winter values

15   of TC_{NF} and levoglucosan. The apportioned fossil fuel carbon fraction from the $F^{14}C$ and levoglucosan method (TC_{FF}) is estimated to 20 % of TC throughout the year (Fig. 6), this is in good agreement with the previous studies from Vavihill measurement station (Genberg et al., 2011;Yttri et al., 2011a). However, there was a significant difference in fossil carbon apportioned between the two methods (p=0.04). Throughout the year, the aethalometer model overestimates the fossil carbon by a factor 1.3 compared to $F^{14}C$ and levoglucosan source apportionment. Further, TC_{FF} displays a better agreement with

20   NO_X than the aethalometer model derived CM_{FF} (R^2=0.15; p<0.001 vs. R^2=0.06; p=0.007), indicating a more accurate apportionment of fossil carbon using $F^{14}C$.

Apportioned wood burning, TC_{WB}, showed a clear intra-annual variability with high carbon contribution during winter (60 %) and low during summer (9 %), this is similar to the aethalometer model, CM_{WB}, results. For the whole year, there was no significant difference in apportioned wood burning carbonaceous aerosol between the two methods (p=0.8).

25   The biogenic carbon fraction, TC_{Bio}, is dominating TC during summer (75 %), but is not negligible during winter (13 %, Fig. 6) in the radiocarbon and levoglucosan model. Apportioned biogenic carbon was in good agreement between the methods, i.e. no significant differences between the methods were observed for the whole year data (p=0.32).

Thus, with respect to apportioned wood burning and biogenic carbonaceous aerosol, the aethalometer model setup presented in this paper shows good agreement with the radiocarbon and levoglucosan model. However, it is interesting to investigate

30   two other possible setups of the model, for a possibly more accurate aethalometer model source apportionment of the fossil carbon: A) to include the removed outliers in the linear regressions used to derive C_1 and C_2; B) to solve Eq. 9 with a bilinear fit, as originally proposed by Sandradewi et al. (2008a).

A) Including removed outliers would result in C_1 and C_2 parameters of 371 047 µg m^{-2} and 88 188 µg m^{-2}, respectively. The statistics for both linear regressions would improve, the R^2 for C_1 would for instance increase from 0.29 to 0.67. However, increasing the C_1 parameter by a factor of 1.7 (from 214 467 to 371 047 µg m^{-2}) would result in large discrepancies compared to the $F^{14}C$ and levoglucosan method. In general, for the whole measurement campaign, the fossil fuel contribution by the aethalometer model would be overestimated by a factor 2.4 while the biogenic mass contribution would be underestimated by a factor 1.7 compared to radiocarbon and levoglucosan source apportionment. The CM_{WB} contribution to TC would be underestimated by a factor 1.3 compared to TC_{WB}.

B) When we derived the C_1 and C_2 parameters by solving Eq. 9 as a multilinear fit (letting CM_{Bio} be a fixed intercept) C_1 and C_2 were determined to 497 279 µg m^{-2} and 68 859 µg m^{-2}, respectively. CM_{Bio} was fixed to -0.103 µg m^{-3}. Hence, the multilinear solution provides a C_1 parameter that is approximately 2.2 times larger than the C_1 obtained by the current linear regression of Eq. 10, and a C_2 parameter that is 1.7 times smaller than the C_2 obtained by Eq. 11. The multilinear aethalometer model solution should ideally be compared to radiocarbon and levoglucosan source apportionment results derived from Eq. 18 were *a* was derived from a linear fit of winter data with an allowed intercept, i.e. biogenic carbon is allowed in TC_{NF}. *a* is then determined to 7.16 with an intercept of 0.17. This approach will lead to an overestimation of CM_{FF} by a factor 3.2 compared to TC_{FF} and an underestimation of CM_{WB} by a factor 1.5 compared to TC_{WB}. Thus, a bilinear solution to Eq. 9 would increase the discrepancy between the aethalometer model and the radiocarbon and levoglucosan source apportionment method.

Furthermore, we performed a sensitivity analysis with the aim of studying the impact of increased or decreased biogenic carbon during winter on the derived C_1 and C_2 parameters and the resulting source apportionment. In Eq. 10 and 11 we increased and decreased the TC by +5 % and -5 %, respectively, without changing any of the b_{abs} parameters. Thus, the induced change in TC will be analogous to changes in biogenic carbon concentration, assuming that this fraction is non-light absorbing. A 5 % change in TC led to a corresponding 5 % change in the derived C_1 and C_2 parameters. Hence, increasing the non-light absorbing TC would result in increased apportionment of TC into fossil fuel and wood burning, this would in turn result in a decreased apportionment to biogenic carbon. Increased concentrations of non-light absorbing carbon by 5 % during winter would result in an even larger annual significant overestimation of fossil fuel carbon by the aethalometer model (a factor 1.4 higher, p=0.007) in comparison to the $F^{14}C$ and levoglucosan source apportionment. However, this 5 % increase would not result in a significantly different aethalometer model apportionment of wood burning and biogenic carbon in comparison to the $F^{14}C$ and levoglucosan method. On the other hand, a 5 % decrease of non-light absorbing carbon would lead to better agreement in apportioned fossil fuel carbon between the aethalometer model and the $F^{14}C$ and levoglucosan method. For the whole year, there would be no significant difference in apportioned fossil fuel carbon by the two methods (p=0.137). Also, apportioned wood burning and biogenic carbon would not show any significant differences between the methods (p=0.941 and p=0.943, respectively). Thus, the presence of non-light absorbing carbon might explain the observed significant difference in apportioned fossil fuel carbon (Fig. 6). We conclude that the model is sensitive to non-light absorbing carbon and that this fraction needs to be minimized in order for the model to function correctly.

3.5 Air mass trajectory analysis

For the whole measurement period, air masses arriving from SW dominated and contributed with 35 % of the incoming air masses. The remaining contributions of the NW, SE and NE sectors were 32, 17 and 16 %, respectively. Air masses arriving from SE were dominating during the fall (31 %) and were more polluted than air masses from other directions. CM_{FF}, CM_{WB}, levoglucosan and PM_{10} all increased with increasing fraction of incoming SE winds (p<0.01). The elevated PM levels from this area can be explained by a large fraction of densely populated land and with air dominated by high pressure systems inhibiting vertical mixing with cleaner air.

Increasing fraction of NE air masses correlated with increasing amount of biogenic aerosol (CM_{Bio}, p<0.01), while other types of PM were low. $F^{14}C$ also increased with NE fraction (p=0.03), supporting the impact of biogenic sources from this direction. This relation seems geographically sound, due to the relatively large and sparsely populated land area. Further, since the abundance of incoming NE air masses was low during winter (10 %), the possible disturbance of biogenic carbon in the aethalometer model should have been minimized.

The NW direction from Vavihill is dominated by the North Atlantic, North Sea and Norwegian Sea which are displayed in the results; all carbonaceous PM species tend to decrease with increasing fraction of incoming air mass from NW (p<0.01). Air masses arriving from this region can thus be considered relatively clean, this direction dominated during the summer (43 %). Finally, SW air masses tend to carry NO_X, but no carbonaceous PM species correlates with this air mass direction. Increased fraction of SW air masses correlates to increased precipitation (p<0.01), hence it is possible that SW-related precipitation decreases carbonaceous PM through wet deposition while leaving the NO_X unaffected.

These results are in line with the findings of Kristensson et al. (2008) who found that air masses from north were in general cleaner than air masses from continental Europe.

3.6 Source apportionment uncertainty estimation by the propagation of errors

Many source apportionment studies omit comprehensive uncertainty estimations. This can have severe impacts for decision and policymaking based on the studies. In the present study, an attempt to approximate measurement and linear estimation uncertainty on the calculated fractions of fossil fuel (CM_{FF}), wood burning (CM_{WB}) and biogenic (CM_{Bio}) carbonaceous aerosol was conducted by the recommendations of Henry et al. (1984). The approach of propagation of errors was used and the most obvious uncertainties were estimated and summarized. Aethalometer measurements have been suggested to give an uncertainty of 5 % to absorption coefficients (Hansen, 2005). However, recent work by Zanatta et al. (2016) proposes an uncertainty of 35 % to aethalometer derived absorption coefficients. We select the more conservative uncertainty of 35 % for this analysis. AAE_{WB} and AAE_{FF} are associated with uncertainties of 30 % and 10 %, respectively (Table 1). It should be noticed that previous studies support our selection of AAEs (Massabo et al., 2015;Sandradewi et al., 2008b). The measured values of OC, EC and TC are associated with an uncertainty of 17 % (Cavalli et al., 2016). Finally, the estimation of the C_1 and C_2 parameters were associated with uncertainties of 31 % and 18 %, respectively. Considering that the fraction of fossil

fuel combustion aerosol is based on aethalometer measurements (absorption coefficients), AAE_{FF}, TOA (OC, EC, TC) and C_1, this parameter get a total uncertainty of 41 %. Similarly, for the fraction wood burning aerosol, we base the total uncertainty on aethalometer measurements, AAE_{WB}, TOA and C_2. The overall uncertainty is then estimated to 42 %. Despite the relatively high estimated uncertainty, it is worth noting that the CM_{WB} agreement with levoglucosan was satisfactory (Fig. 5). Finally, we base the biogenic aerosol (CM_{Bio}) uncertainty on aethalometer measurements, AAE_{FF}, AAE_{WB}, C_1, C_2 and TOA. The biogenic carbonaceous aerosol fraction then reaches a total uncertainty of 50 %.

4 Conclusions

The aethalometer model offers fast, inexpensive apportionment of the carbonaceous aerosol. The accuracy and robustness of the model principle has previously been questioned. In this study we propose a small modification to the aethalometer model which enables apportioned non-absorbing carbon, here assumed to be biogenic carbon, to vary. Propagation of errors showed that fossil, wood burning and biogenic carbonaceous aerosol quantification by the aethalometer model may be highly uncertain. Nevertheless, we show that the model works well for a whole year source apportionment for quantifying wood burning and variable biogenic carbonaceous aerosol at a rural site in southern Sweden, as there was a good agreement between aethalometer model and the radiocarbon and levoglucosan source apportionment. The aethalometer model overestimated the fossil carbonaceous aerosol compared to the radiocarbon and levoglucosan method, which may be explained by possible interference of non-light absorbing biogenic carbon during winter. However, relating aerosol light absorption to carbon mass concentration by a bilinear solution or including statistically determined outliers resulted in even larger discrepancies between the two methods. Future studies are needed to investigate the repeatability of our proposed modified aethalometer model.

5 Data availability

All data are accessible through the supporting information.

Author contributions

Johan Martinsson designed the study and analysed all data. Hafiz Abdul Azeem conducted levoglucosan analysis. Moa Sporre generated the HYSPLIT results. Erik Ahlberg and Emilie Öström were involved in the aerosol sampling. Adam Kristensson, Erik Swietlicki, Kristina Eriksson Stenström and Robert Bergström assisted in the writing process.

Acknowledgements

This work was supported by The Swedish Research Council FORMAS (project 2011-743). The authors acknowledge research technician Mattias Olsson for graphitization and analysis of radiocarbon in filter samples.

References

5   Barregard, L., Sallsten, G., Gustafson, P., Andersson, L., Johansson, L., Basu, S., and Stigendal, L.: Experimental exposure to wood-smoke particles in healthy humans: Effects on markers of inflammation, coagulation, and lipid peroxidation, Inhal. Toxicol., 18, 845-853, 10.1080/08958370600685798, 2006.

Benbrahim-Tallaa, L., Baan, R. A., Grosse, Y., Lauby-Secretan, B., El Ghissassi, F., Bouvard, V., Guha, N., Loomis, D.,
10 Straif, K., and Workin, I. A. R. C. M.: Carcinogenicity of diesel-engine and gasoline-engine exhausts and some nitroarenes, Lancet. Oncol., 13, 663-664, 10.1016/S1470-2045(12)70280-2, 2012.

Bond, T. C., and Bergstrom, R. W.: Light absorption by carbonaceous particles: An investigative review, Aerosol. Sci. Tech., 40, 27-67, 10.1080/02786820500421521, 2006.

Bond, T. C., Doherty, S. J., Fahey, D. W., Forster, P. M., Berntsen, T., DeAngelo, B. J., Flanner, M. G., Ghan, S., Karcher, B., Koch, D., Kinne, S., Kondo, Y., Quinn, P. K., Sarofim, M. C., Schultz, M. G., Schulz, M., Venkataraman, C., Zhang, H., Zhang, S., Bellouin, N., Guttikunda, S. K., Hopke, P. K., Jacobson, M. Z., Kaiser, J. W., Klimont, Z., Lohmann, U., Schwarz, J. P., Shindell, D., Storelvmo, T., Warren, S. G., and Zender, C. S.: Bounding the role of black carbon in the
20 climate system: A scientific assessment, J. Geophys. Res.-Atmos., 118, 5380-5552, 10.1002/jgrd.50171, 2013.

Bonvalot, L., Tuna, T., Fagault, Y., Jaffrezo, J. L., Jacob, V., Chevrier, F., and Bard, E.: Estimating contributions from biomass burning, fossil fuel combustion, and biogenic carbon to carbonaceous aerosols in the Valley of Chamonix: a dual approach based on radiocarbon and levoglucosan, Atmos. Chem. Phys., 16, 13753-13772, 10.5194/acp-16-13753-2016,
25 2016.

Calvo, A. I., Martins, V., Nunes, T., Duarte, M., Hillamo, R., Teinilae, K., Pont, V., Castro, A., Fraile, R., Tarelho, L., and Alves, C.: Residential wood combustion in two domestic devices: Relationship of different parameters throughout the combustion cycle, Atmos. Environ., 116, 72-82, 10.1016/j.atmosenv.2015.06.012, 2015.

Cavalli, F., Viana, M., Yttri, K. E., Genberg, J., and Putaud, J. P.: Toward a standardised thermal-optical protocol for measuring atmospheric organic and elemental carbon: the EUSAAR protocol, Atmos. Meas. Tech., 3, 79-89, 2010.

Cavalli, F., Alastuey, A., Areskoug, H., Ceburnis, D., Cech, J., Genberg, J., Harrison, R. M., Jaffrezo, J. L., Kiss, G., Laj, P.,
35 Mihalopoulos, N., Perez, N., Quincey, P., Schwartz, J., Sellegri, K., Spindler, G., Swietlicki, E., Theodosi, C., Yttri, K. E., Aas, W., and Putaud, J. P.: A European aerosol phenomenology -4: Harmonized concentrations of carbonaceous aerosol at 10 regional background sites across Europe, Atmos. Environ., 144, 133-145, http://dx.doi.org/10.1016/j.atmosenv.2016.07.050, 2016.

40 Clarke, A., McNaughton, C., Kapustin, V., Shinozuka, Y., Howell, S., Dibb, J., Zhou, J., Anderson, B., Brekhovskikh, V., Turner, H., and Pinkerton, M.: Biomass burning and pollution aerosol over North America: Organic components and their influence on spectral optical properties and humidification response, J. Geophys. Res.-Atmos., 112, Artn D12s1810.1029/2006jd007777, 2007.

Day, D. E., Hand, J. L., Carrico, C. M., Engling, G., and Malm, W. C.: Humidification factors from laboratory studies of fresh smoke from biomass fuels, J. Geophys. Res.-Atmos., 111, Artn D2220210.1029/2006jd007221, 2006.

Doherty, S. J., Warren, S. G., Grenfell, T. C., Clarke, A. D., and Brandt, R. E.: Light-absorbing impurities in Arctic snow, Atmos. Chem. Phys., 10, 11647-11680, 10.5194/acp-10-11647-2010, 2010.

Draxier, R. R., and Hess, G. D.: An overview of the HYSPLIT_4 modelling system for trajectories, dispersion and deposition, Aust. Meteorol. Mag., 47, 295-308, 1998.

Drinovec, L., Mocnik, G., Zotter, P., Prevot, A. S. H., Ruckstuhl, C., Coz, E., Rupakheti, M., Sciare, J., Müller, T., Wiedensohler, A., and Hansen, A. D. A.: The "dual-spot" Aethalometer: an improved measurement of aerosol black carbon with real-time loading compensation, Atmos. Meas. Tech., 8, 1965-1979, 10.5194/amt-8-1965-2015, 2015.

EEA.: Renewable energy in gross inland energy consumption: http://www.eea.europa.eu/data-and-maps/indicators/renewable-primary-energy-consumption-3/assessment, 2015.

Eriksson, A. C., Nordin, E. Z., Nyström, R., Pettersson, E., Swietlicki, E., Bergvall, C., Westerholm, R., Boman, C., and Pagels, J. H.: Particulate PAH Emissions from Residential Biomass Combustion: Time-Resolved Analysis with Aerosol Mass Spectrometry, Environ. Sci. Technol., 48, 7143-7150, 10.1021/es500486j, 2014.

Fabbri, D., Marynowski, L., Fabianska, M. J., Zaton, M., and Simoneit, B. R. T.: Levoglucosan and other cellulose markers in pyrolysates of miocene lignites: Geochemical and environmental implications, Environ. Sci. Technol., 42, 2957-2963, 10.1021/es7021472, 2008.

Favez, O., Cachier, H., Sciare, J., Sarda-Esteve, R., and Martinon, L.: Evidence for a significant contribution of wood burning aerosols to PM2.5 during the winter season in Paris, France, Atmos. Environ., 43, 3640-3644, 10.1016/j.atmosenv.2009.04.035, 2009.

Favez, O., El Haddad, I., Piot, C., Boreave, A., Abidi, E., Marchand, N., Jaffrezo, J. L., Besombes, J. L., Personnaz, M. B., Sciare, J., Wortham, H., George, C., and D'Anna, B.: Inter-comparison of source apportionment models for the estimation of wood burning aerosols during wintertime in an Alpine city (Grenoble, France), Atmos. Chem. Phys., 10, 5295-5314, 10.5194/acp-10-5295-2010, 2010.

Fuller, G. W., Tremper, A. H., Baker, T. D., Yttri, K. E., and Butterfield, D.: Contribution of wood burning to PM10 in London, Atmos. Environ., 87, 87-94, 10.1016/j.atmosenv.2013.12.037, 2014.

Fuzzi, S., Baltensperger, U., Carslaw, K., Decesari, S., van Der Gon, H. D., Facchini, M. C., Fowler, D., Koren, I., Langford, B., Lohmann, U., Nemitz, E., Pandis, S., Riipinen, I., Rudich, Y., Schaap, M., Slowik, J. G., Spracklen, D. V., Vignati, E., Wild, M., Williams, M., and Gilardoni, S.: Particulate matter, air quality and climate: lessons learned and future needs, Atmos. Chem. Phys., 15, 8217-8299, 10.5194/acp-15-8217-2015, 2015.

Garg, S., Chandra, B. P., Sinha, V., Sarda-Esteve, R., Gros, V., and Sinha, B.: Limitation of the Use of the Absorption Angstrom Exponent for Source Apportionment of Equivalent Black Carbon: a Case Study from the North West Indo-Gangetic Plain, Environ. Sci. Technol., 50, 814-824, 10.1021/acs.est.5b03868, 2016.

Gelencser, A., May, B., Simpson, D., Sanchez-Ochoa, A., Kasper-Giebl, A., Puxbaum, H., Caseiro, A., Pio, C., and Legrand, M.: Source apportionment of PM2.5 organic aerosol over Europe: Primary/secondary, natural/anthropogenic, and fossil/biogenic origin, J. Geophys. Res.-Atmos., 112, Artn D23s0410.1029/2006jd008094, 2007.

Genberg, J., Stenström, K., Elfman, M., and Olsson, M.: DEVELOPMENT OF GRAPHITIZATION OF μg-SIZED SAMPLES AT LUND UNIVERSITY, Radiocarbon, 52, 1270-1276, 2010.

Genberg, J., Hyder, M., Stenström, K., Bergström, R., Simpson, D., Fors, E. O., Jönsson, J. A., and Swietlicki, E.: Source apportionment of carbonaceous aerosol in southern Sweden, Atmos. Chem. Phys., 11, 11387-11400, 10.5194/acp-11-11387-2011, 2011.

Gilardoni, S., Vignati, E., Cavalli, F., Putaud, J. P., Larsen, B. R., Karl, M., Stenström, K., Genberg, J., Henne, S., and Dentener, F.: Better constraints on sources of carbonaceous aerosols using a combined ^{14}C - macro tracer analysis in a European rural background site, Atmos. Chem. Phys., 11, 5685-5700, 10.5194/acp-11-5685-2011, 2011.

Grahame, T. J., Klemm, R., and Schlesinger, R. B.: Public health and components of particulate matter: The changing assessment of black carbon, J. Air. Waste. Manage., 64, 620-660, 10.1080/10962247.2014.912692, 2014.

Grubbs, F. E.: Sample Criteria for Testing Outlying Observations, Ann. Math. Stat., 21, 27-58, DOI 10.1214/aoms/1177729885, 1950.

Guenther, A., Hewitt, C. N., Erickson, D., Fall, R., Geron, C., Graedel, T., Harley, P., Klinger, L., Lerdau, M., Mckay, W. A., Pierce, T., Scholes, B., Steinbrecher, R., Tallamraju, R., Taylor, J., and Zimmerman, P.: A Global-Model of Natural Volatile Organic-Compound Emissions, J. Geophys. Res.-Atmos., 100, 8873-8892, Doi 10.1029/94jd02950, 1995.

Hansen, A. D. A.: The Aethalometer, manual, Berkeley, California, USA, Magee Scientific., 2005.

Harrison, R. M., Beddows, D. C. S., Hu, L., and Yin, J.: Comparison of methods for evaluation of wood smoke and estimation of UK ambient concentrations, Atmos. Chem. Phys., 12, 8271-8283, 10.5194/acp-12-8271-2012, 2012.

Harrison, R. M., Beddows, D. C. S., Jones, A. M., Calvo, A., Alves, C., and Pio, C.: An evaluation of some issues regarding the use of aethalometers to measure woodsmoke concentrations, Atmos. Environ., 80, 540-548, 10.1016/j.atmosenv.2013.08.026, 2013.

Hedberg, E., and Johansson, C.: Is levoglucosan a suitable quantitative tracer for wood burning? Comparison with receptor modeling on trace elements in Lycksele, Sweden, J. Air. Waste. Manage., 56, 1669-1678, 2006.

Hellborg, R., and Skog, G.: Accelerator mass spectrometry, Mass. Spectrom. Rev., 27, 398-427, 10.1002/mas.20172, 2008.

Hennigan, C. J., Sullivan, A. P., Collett, J. L., and Robinson, A. L.: Levoglucosan stability in biomass burning particles exposed to hydroxyl radicals, Geophys. Res. Lett., 37, Artn L0980610.1029/2010gl043088, 2010.

Henry, R. C., Lewis, C. W., Hopke, P. K., and Williamson, H. J.: Review of Receptor Model Fundamentals, Atmos. Environ., 18, 1507-1515, Doi 10.1016/0004-6981(84)90375-5, 1984.

Herich, H., Hueglin, C., and Buchmann, B.: A 2.5 year's source apportionment study of black carbon from wood burning and fossil fuel combustion at urban and rural sites in Switzerland, Atmos. Meas. Tech., 4, 1409-1420, DOI 10.5194/amt-4-1409-2011, 2011.

Hoek, G., Brunekreef, B., Goldbohm, S., Fischer, P., and van den Brandt, P. A.: Association between mortality and indicators of traffic-related air pollution in the Netherlands: a cohort study, Lancet, 360, 1203-1209, Doi 10.1016/S0140-6736(02)11280-3, 2002.

Hoffmann, D., Tilgner, A., Iinuma, Y., and Herrmann, H.: Atmospheric Stability of Levoglucosan: A Detailed Laboratory and Modeling Study, Environ. Sci. Technol., 44, 694-699, 10.1021/es902476f, 2010.

Iinuma, Y., Brüggemann, E., Gnauk, T., Müller, K., Andreae, M. O., Helas, G., Parmar, R., and Herrmann, H.: Source characterization of biomass burning particles: The combustion of selected European conifers, African hardwood, savanna grass, and German and Indonesian peat, J. Geophys. Res.-Atmos., 112, Artn D0820910.1029/2006jd007120, 2007.

IPCC: Summary for policymakers. In: Climate Change 2013: The Physical Science Basis. Contribution of Working Group I to the Fifth Assessment Report of the Intergovernmental Panel on Climate Change., Cambridge, United Kingdom and New York, NY, USA., 2013.

Jacobson, M. Z.: Isolating nitrated and aromatic aerosols and nitrated aromatic gases as sources of ultraviolet light absorption, J. Geophys. Res.-Atmos., 104, 3527-3542, Doi 10.1029/1998jd100054, 1999.

Jalava, P. I., Salonen, R. O., Nuutinen, K., Pennanen, A. S., Happo, M. S., Tissari, J., Frey, A., Hillamo, R., Jokiniemi, J., and Hirvonen, M. R.: Effect of combustion condition on cytotoxic and inflammatory activity of residential wood combustion particles, Atmos. Environ., 44, 1691-1698, 10.1016/j.atmosenv.2009.12.034, 2010.

Kirchstetter, T. W., Novakov, T., and Hobbs, P. V.: Evidence that the spectral dependence of light absorption by aerosols is affected by organic carbon, J. Geophys. Res.-Atmos., 109, Artn D21208Doi 10.1029/2004jd004999, 2004.

Kirchstetter, T. W., and Thatcher, T. L.: Contribution of organic carbon to wood smoke particulate matter absorption of solar radiation, Atmos. Chem. Phys., 12, 6067-6072, DOI 10.5194/acp-12-6067-2012, 2012.

Kristensson, A., Dal Maso, M., Swietlicki, E., Hussein, T., Zhou, J., Kerminen, V. M., and Kulmala, M.: Characterization of new particle formation events at a background site in Southern Sweden: relation to air mass history, Tellus B, 60, 330-344, 10.1111/j.1600-0889.2008.00345.x, 2008.

Kristensson, A., Rissler, J., Löndahl, J., Johansson, C., and Swietlicki, E.: Size-Resolved Respiratory Tract Deposition of Sub-Micrometer Aerosol Particles in a Residential Area with Wintertime Wood Combustion, Aerosol Air Qual. Res., 13, 24-35, 10.4209/aaqr.2010.04.0025, 2013.

Lack, D. A., Bahreni, R., Langridge, J. M., Gilman, J. B., and Middlebrook, A. M.: Brown carbon absorption linked to organic mass tracers in biomass burning particles, Atmos. Chem. Phys., 13, 2415-2422, 10.5194/acp-13-2415-2013, 2013.

Laden, F., Schwartz, J., Speizer, F. E., and Dockery, D. W.: Reduction in fine particulate air pollution and mortality - Extended follow-up of the Harvard six cities study, American Journal of Respiratory and Critical Care Medicine, 173, 667-672, 10.1164/rccm.200503-443OC, 2006.

Laskin, A., Laskin, J., and Nizkorodov, S. A.: Chemistry of Atmospheric Brown Carbon, Chem. Rev., 115, 4335-4382, 10.1021/cr5006167, 2015.

Lewis, K., Arnott, W. P., Moosmüller, H., and Wold, C. E.: Strong spectral variation of biomass smoke light absorption and single scattering albedo observed with a novel dual-wavelength photoacoustic instrument, J. Geophys. Res.-Atmos., 113, Artn D1620310.1029/2007jd009699, 2008.

Martinsson, J., Eriksson, A. C., Nielsen, I. E., Malmborg, V. B., Ahlberg, E., Andersen, C., Lindgren, R., Nyström, R., Nordin, E. Z., Brune, W. H., Svenningsson, B., Swietlicki, E., Boman, C., and Pagels, J. H.: Impacts of Combustion Conditions and Photochemical Processing on the Light Absorption of Biomass Combustion Aerosol, Environ. Sci. Technol., 49, 14663-14671, 10.1021/acs.est.5b03205, 2015.

Massabo, D., Caponi, L., Bernardoni, V., Bove, M. C., Brotto, P., Calzolai, G., Cassola, F., Chiari, M., Fedi, M. E., Fermo, P., Giannoni, M., Lucarelli, F., Nava, S., Piazzalunga, A., Valli, G., Vecchi, R., and Prati, P.: Multi-wavelength optical determination of black and brown carbon in atmospheric aerosols, Atmos. Environ., 108, 1-12, 10.1016/j.atmosenv.2015.02.058, 2015.

May, A. A., Saleh, R., Hennigan, C. J., Donahue, N. M., and Robinson, A. L.: Volatility of Organic Molecular Markers Used for Source Apportionment Analysis: Measurements and Implications for Atmospheric Lifetime, Environ. Sci. Technol., 46, 12435-12444, 10.1021/es302276t, 2012.

Mohr, C., Lopez-Hilfiker, F. D., Zotter, P., Prevot, A. S. H., Xu, L., Ng, N. L., Herndon, S. C., Williams, L. R., Franklin, J. P., Zahniser, M. S., Worsnop, D. R., Knighton, W. B., Aiken, A. C., Gorkowski, K. J., Dubey, M. K., Allan, J. D., and Thornton, J. A.: Contribution of Nitrated Phenols to Wood Burning Brown Carbon Light Absorption in Detling, United Kingdom during Winter Time, Environ. Sci. Technol., 47, 6316-6324, Doi 10.1021/Es400683v, 2013.

Naeher, L. P., Brauer, M., Lipsett, M., Zelikoff, J. T., Simpson, C. D., Koenig, J. Q., and Smith, K. R.: Woodsmoke health effects: A review, Inhal. Toxicol., 19, 67-106, Doi 10.1080/08958370600985875, 2007.

Pope, C. A., and Dockery, D. W.: Health effects of fine particulate air pollution: Lines that connect, J. Air. Waste Manage., 56, 709-742, 2006.

Rafter, T. A., and Fergusson, G. J.: Atom Bomb Effect - Recent Increase of Carbon-14 Content of the Atmosphere and Biosphere, Science, 126, 557-558, DOI 10.1126/science.126.3273.557, 1957.

Reimer, P. J., Brown, T. A., and Reimer, R. W.: Discussion: Reporting and calibration of post-bomb ^{14}C data, Radiocarbon, 46, 1299-1304, 2004.

Rissler, J., Nordin, E. Z., Eriksson, A. C., Nilsson, P. T., Frosch, M., Sporre, M. K., Wierzbicka, A., Svenningsson, B., Löndahl, J., Messing, M. E., Sjögren, S., Hemmingsen, J. G., Loft, S., Pagels, J. H., and Swietlicki, E.: Effective Density and Mixing State of Aerosol Particles in a Near-Traffic Urban Environment, Environ. Sci. Technol., 48, 6300-6308, 10.1021/es5000353, 2014.

Roden, C. A., Bond, T. C., Conway, S., Benjamin, A., and Pinel, O.: Emission factors and real-time optical properties of particles emitted from traditional wood burning cookstoves, Environ. Sci. Technol., 40, 6750-6757, 10.1021/es052080i, 2006.

Saleh, R., Hennigan, C. J., McMeeking, G. R., Chuang, W. K., Robinson, E. S., Coe, H., Donahue, N. M., and Robinson, A. L.: Absorptivity of brown carbon in fresh and photo-chemically aged biomass-burning emissions, Atmos. Chem. Phys., 13, 7683-7693, DOI 10.5194/acp-13-7683-2013, 2013.

Saleh, R., Robinson, E. S., Tkacik, D. S., Ahern, A. T., Liu, S., Aiken, A. C., Sullivan, R. C., Presto, A. A., Dubey, M. K., Yokelson, R. J., Donahue, N. M., and Robinson, A. L.: Brownness of organics in aerosols from biomass burning linked to their black carbon content, Nat. Geosci., 7, 647-650, Doi 10.1038/Ngeo2220, 2014.

Salvi, S., Blomberg, A., Rudell, B., Kelly, F., Sandström, T., Holgate, S. T., and Frew, A.: Acute inflammatory responses in the airways and peripheral blood after short-term exposure to diesel exhaust in healthy human volunteers, American Journal of Respiratory and Critical Care Medicine, 159, 702-709, 1999.

Sandradewi, J., Prevot, A. S. H., Szidat, S., Perron, N., Alfarra, M. R., Lanz, V. A., Weingartner, E., and Baltensperger, U.: Using aerosol light absorption measurements for the quantitative determination of wood burning and traffic emission contributions to particulate matter, Environ. Sci. Technol., 42, 3316-3323, Doi 10.1021/Es702253m, 2008a.

5   Sandradewi, J., Prevot, A. S. H., Weingartner, E., Schmidhauser, R., Gysel, M., and Baltensperger, U.: A study of wood burning and traffic aerosols in an Alpine valley using a multi-wavelength Aethalometer, Atmos. Environ., 42, 101-112, DOI 10.1016/j.atmosenv.2007.09.034, 2008b.

Schmidl, C., Marr, L. L., Caseiro, A., Kotianova, P., Berner, A., Bauer, H., Kasper-Giebl, A., and Puxbaum, H.: Chemical
10   characterisation of fine particle emissions from wood stove combustion of common woods growing in mid-European Alpine regions, Atmos. Environ., 42, 126-141, 10.1016/j.atmosenv.2007.09.028, 2008.

Schnaiter, M., Horvath, H., Mohler, O., Naumann, K. H., Saathoff, H., and Schock, O. W.: UV-VIS-NIR spectral optical properties of soot and soot-containing aerosols, J. Aerosol Sci., 34, 1421-1444, 10.1016/S0021-8502(03)00361-6, 2003.
15
Sehlstedt, M., Dove, R., Boman, C., Pagels, J., Swietlicki, E., Löndahl, J., Westerholm, R., Bosson, J., Barath, S., Behndig, A. F., Pourazar, J., Sandström, T., Mudway, I. S., and Blomberg, A.: Antioxidant airway responses following experimental exposure to wood smoke in man, Part. Fibre Toxicol., 7, Artn 2110.1186/1743-8977-7-21, 2010.

20   Simoneit, B. R. T.: Biomass burning - A review of organic tracers for smoke from incomplete combustion, Appl. Geochem., 17, 129-162, Pii S0883-2927(01)00061-0Doi 10.1016/S0883-2927(01)00061-0, 2002.

Skog, G.: The single stage AMS machine at Lund University: Status report, Nucl. Instrum. Meth. B, 259, 1-6, 10.1016/j.nimb.2007.01.190, 2007.
25
Skog, G., Rundgren, M., and Sköld, P.: Status of the Single Stage AMS machine at Lund University after 4 years of operation, Nucl. Instrum. Meth. B, 268, 895-897, 10.1016/j.nimb.2009.10.058, 2010.

Stein, A. F., Draxler, R. R., Rolph, G. D., Stunder, B. J. B., Cohen, M. D., and Ngan, F.: Noaa's Hysplit Atmospheric
30   Transport and Dispersion Modeling System, B Am. Meteorol. Soc., 96, 2059-2077, 10.1175/Bams-D-14-00110.1, 2015.

Suess, H. E.: Radiocarbon Concentration in Modern Wood, Science, 122, 415-417, DOI 10.1126/science.122.3166.415-a, 1955.

35   Szidat, S., Jenk, T. M., Synal, H. A., Kalberer, M., Wacker, L., Hajdas, I., Kasper-Giebl, A., and Baltensperger, U.: Contributions of fossil fuel, biomass-burning, and biogenic emissions to carbonaceous aerosols in Zurich as traced by ^{14}C, J. Geophys. Res.-Atmos., 111, Artn D0720610.1029/2005jd006590, 2006.

Unosson, J., Blomberg, A., Sandström, T., Muala, A., Boman, C., Nyström, R., Westerholm, R., Mills, N. L., Newby, D. E.,
40   Langrish, J. P., and Bosson, J. A.: Exposure to wood smoke increases arterial stiffness and decreases heart rate variability in humans, Part. Fibre Toxicol., 10, Artn 2010.1186/1743-8977-10-20, 2013.

van der Gon, H. A. C. D., Bergström, R., Fountoukis, C., Johansson, C., Pandis, S. N., Simpson, D., and Visschedijk, A. J. H.: Particulate emissions from residential wood combustion in Europe revised estimates and an evaluation, Atmos. Chem.
45   Phys., 15, 6503-6519, 10.5194/acp-15-6503-2015, 2015.

Wang, Y. G., Hopke, P. K., Rattigan, O. V., Xia, X. Y., Chalupa, D. C., and Utell, M. J.: Characterization of Residential Wood Combustion Particles Using the Two-Wavelength Aethalometer, Environ. Sci. Technol., 45, 7387-7393, 10.1021/es2013984, 2011.
50

Weingartner, E., Saathoff, H., Schnaiter, M., Streit, N., Bitnar, B., and Baltensperger, U.: Absorption of light by soot particles: determination of the absorption coefficient by means of aethalometers, J. Aerosol Sci., 34, 1445-1463, Doi 10.1016/S0021-8502(03)00359-8, 2003.

5   Wu, J., Hu, R., Yue, J., Yang, Z., and Zhang, L.: Study on the Derivatization Process Using N-O-bis(trimethylsilyl)-trifluoroacetamide, N-(tert-butyldimethylsilyl)-N-methyltrifluoroacetamide, Trimethylsilyldiazomethane for the Determination of Fecal Sterols by Gas Chromatography-Mass Spectrometry, International Journal of Chemical, Molecular, Nuclear, Materials and Metallurgical Engineering, 2, 175-178, 2008.

10 Yttri, K. E., Simpson, D., Nojgaard, J. K., Kristensen, K., Genberg, J., Stenström, K., Swietlicki, E., Hillamo, R., Aurela, M., Bauer, H., Offenberg, J. H., Jaoui, M., Dye, C., Eckhardt, S., Burkhart, J. F., Stohl, A., and Glasius, M.: Source apportionment of the summer time carbonaceous aerosol at Nordic rural background sites, Atmos. Chem. Phys., 11, 13339-13357, 10.5194/acp-11-13339-2011, 2011a.

15 Yttri, K. E., Simpson, D., Stenström, K., Puxbaum, H., and Svendby, T.: Source apportionment of the carbonaceous aerosol in Norway - quantitative estimates based on ^{14}C, thermal-optical and organic tracer analysis, Atmos Chem Phys, 11, 9375-9394, 10.5194/acp-11-9375-2011, 2011b.

Yttri, K. E., Schnelle-Kreis, J., Maenhaut, W., Abbaszade, G., Alves, C., Bjerke, A., Bonnier, N., Bossi, R., Claeys, M., Dye, 20 C., Evtyugina, M., Garcia-Gacio, D., Hillamo, R., Hoffer, A., Hyder, M., Iinuma, Y., Jaffrezo, J. L., Kasper-Giebl, A., Kiss, G., Lopez-Mahia, P. L., Pio, C., Piot, C., Ramirez-Santa-Cruz, C., Sciare, J., Teinila, K., Vermeylen, R., Vicente, A., and Zimmermann, R.: An intercomparison study of analytical methods used for quantification of levoglucosan in ambient aerosol filter samples, Atmos. Meas. Tech., 8, 125-147, 10.5194/amt-8-125-2015, 2015.

25 Zanatta, M., Gysel, M., Bukowiecki, N., Müller, T., Weingartner, E., Areskoug, H., Fiebig, M., Yttri, K. E., Mihalopoulos, N., Kouvarakis, G. N., Beddows, D., Harrison, R. M., Cavalli, F., Putaud, J. P., Spindler, G., Wiedensohler, A., Alastuey, A., Pandolfi, M., Sellegri, K., Swietlicki, E., Jaffrezo, J. L., Baltensperger, U., and Laj, P.: A European aerosol phenomenology-5: Climatology of black carbon optical properties at 9 regional background sites across Europe, Atmos. Environ., 145, 346-364, http://dx.doi.org/10.1016/j.atmosenv.2016.09.35, 2016.
30
Zhao, R., Mungall, E. L., Lee, A. K. Y., Aljawhary, D., and Abbatt, J. P. D.: Aqueous-phase photooxidation of levoglucosan - a mechanistic study using aerosol time-of-flight chemical ionization mass spectrometry (Aerosol ToF-CIMS), Atmos. Chem. Phys., 14, 9695-9706, 10.5194/acp-14-9695-2014, 2014.

35 Zotter, P., Herich, H., Gysel, M., El-Haddad, I., Zhang, Y., Mocnik, G., Hüglin, C., Baltensperger, U., Szidat, S., and Prevot, A. S. H.: Evaluation of the Ångström exponents for traffic and wood burning in the Aethalometer based source apportionment using radiocarbon measurements of ambient aerosol, Atmos. Chem. Phys. Discuss., doi:10.5194/acp-2016-621, 2016.

40

Table 1: Values of AAE$_{FF}$ and AAE$_{WB}$ derived from reference emission inventories.

AAE$_{FF}$	Spectral region	AAE$_{WB}$	Spectral region	References
1	470-660nm	2.1	470-660nm	(Clarke et al., 2007)
		1.45	UV-IR	(Day et al., 2006)
		1.4	UV-IR	(Garg et al., 2016)
0.9	UV-IR	2.5	UV-IR	(Kirchstetter et al., 2004)
		1.9	UV-IR	(Kirchstetter and Thatcher, 2012)
		1.75	UV-IR	(Lewis et al., 2008)
		1.3	UV-IR	(Martinsson et al., 2015)
		1.3	467-660nm	(Roden et al., 2006)
		1.6	UV-IR	(Saleh et al., 2013)
		2.8	UV-IR	(Sandradewi et al., 2008b)
1.1	450-700nm			(Schnaiter et al., 2003)

Table 2: Site specific mass absorption coefficients (MAC) from the Vavihill measurement station. Values were obtained by linear regression analysis of measured absorption coefficients and elemental carbon (EC) concentrations. The slope is equivalent to $\sigma_{abs}(\lambda)$. Uncertainties are represented by standard errors (N=123).

λ (nm)	$\sigma_{abs}(\lambda)$ ($m^2\ g^{-1}$)
370	41.21 ± 1.00
470	29.06 ± 0.96
520	24.78 ± 0.80
590	21.29 ± 0.68
660	17.57 ± 0.55
880	12.64 ± 0.39
950	11.93 ± 0.37

Table 3: Definition of wind directions of incoming air masses.

Direction	Degrees (°)
Northeast (NE)	0-90
Southeast (SE)	90-180
Southwest (SW)	180-270
Northwest (NW)	270-360

Table 4: Seasonal mean concentrations and contributions to PM$_{10}$ and TC of aethalometer model derived parameters. Uncertainties are given in standard deviations.

Season	Concentration (µg m^{-3})			Contribution to PM$_{10}$ (%)			Contribution to TC (%)		
	CM$_{WB}$	CM$_{FF}$	CM$_{Bio}$	CM$_{WB}$	CM$_{FF}$	CM$_{Bio}$	CM$_{WB}$	CM$_{FF}$	CM$_{Bio}$
Summer	0.07±0.05	0.31±0.19	1.04±0.59	0.6±0.4	2.7±1.1	9.0±2.8	6.1±4.0	21.5±6.9	72.4±6.5
Fall	0.49±0.46	0.62±0.36	1.06±0.68	2.6±1.9	3.7±1.1	6.8±3.4	22.2±14.9	28.4±8.0	49.3±19.8
Winter	0.65±0.53	0.37±0.25	0.13±0.21	5.4±3.5	3.1±1.3	0.9±1.6	56.5±13.3	35.5±9.4	8.0±14.4
Spring	0.51±0.69	0.35±0.30	0.54±0.32	4.9±3.5	3.9±2.1	8.9±9.6	32.3±17.9	25.6±9.0	42.1±22.5
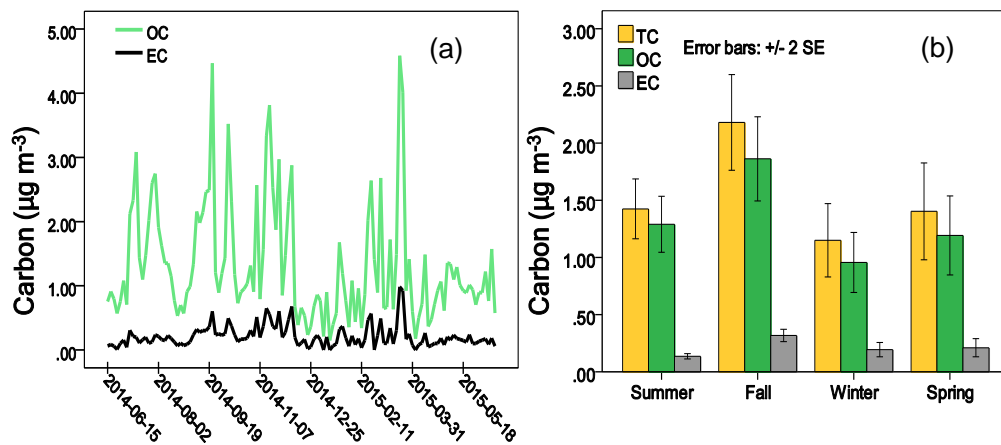
Figure 1: Temporal variations in OC, EC and TC. (a) Shows the temporal variation of OC and EC with a time resolution of 72 h (N=123). (b) Displays the average concentration of TC, OC and EC divided into seasons; summer (N=32), fall (N=30), winter (N=30) and spring (N=31). Error bars display ±2 standard errors (SE).
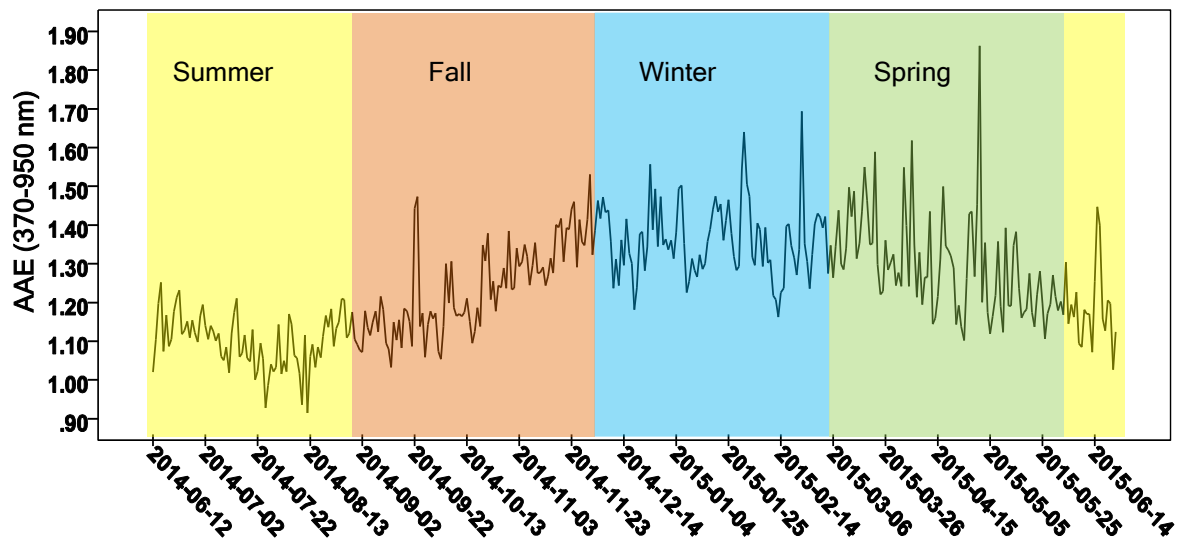
Figure 2: Annual variations in AAE (370-950nm) at the Vavihill measurement station. Colours represent different seasons of the year. N=369.
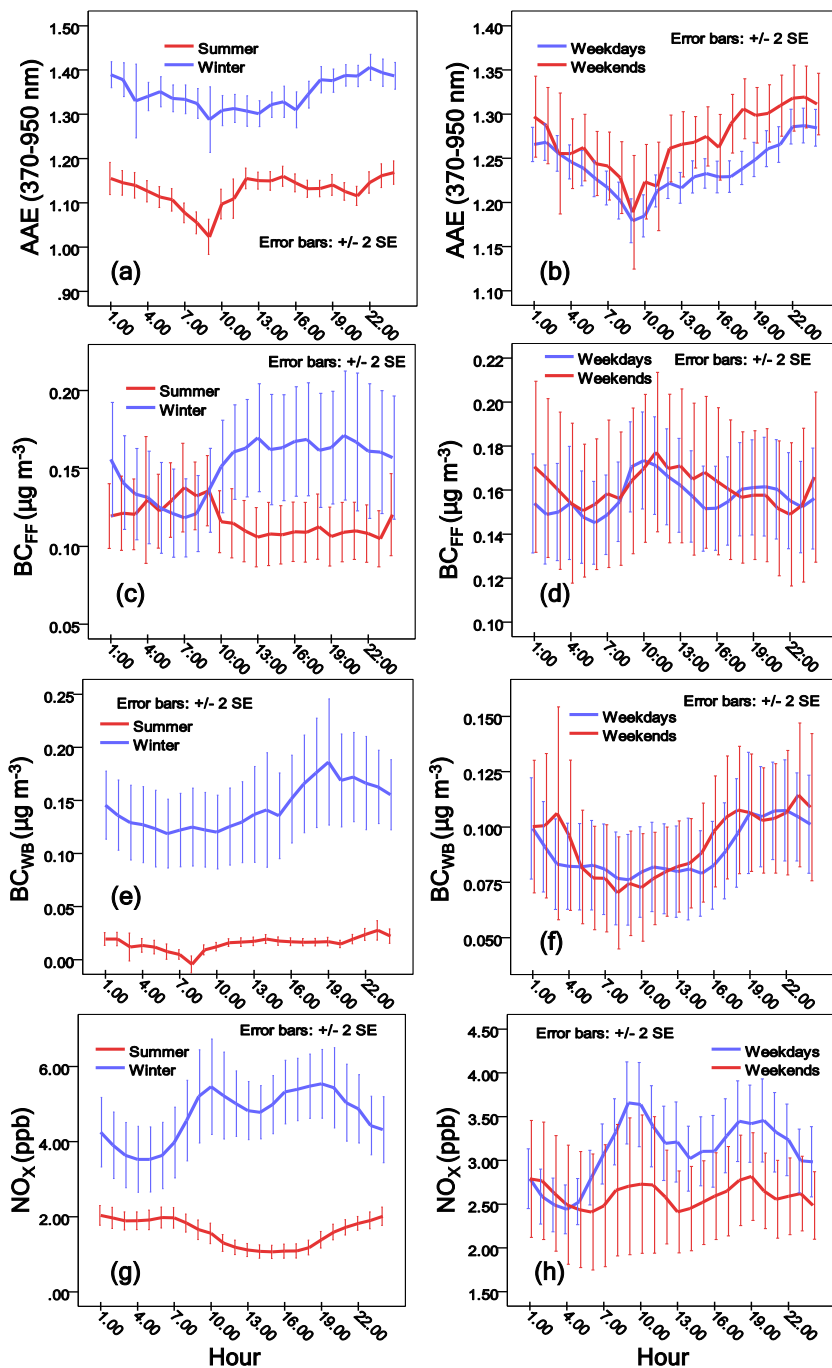
Figure 3: Diurnal variations of AAE (370-950 nm, a-b), BC$_{FF}$ (950 nm, c-d), BC$_{WB}$ (370 nm, e-f) and NO$_X$ (g-h) at the Vavihill measurement station. Figures (a), (c), (e) and (g) represents diurnal differences between summer and winter while Fig. (b), (d), (f), and (h) represents diurnal differences between weekdays (Monday-Friday) and weekends (Saturday-Sunday, including national holidays). Uncertainties are given as 2 times the standard error (SE).
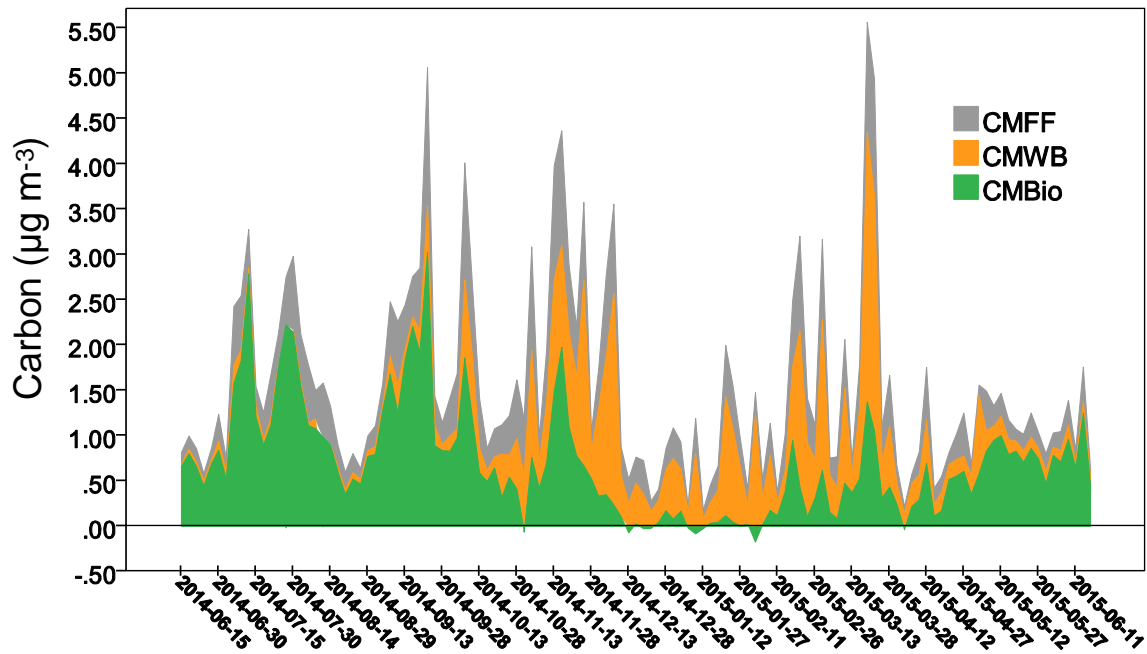
Figure 4: Aethalometer model source apportionment of total carbon from the Vavihill measurement station, June 2014–June 2015. N=123.
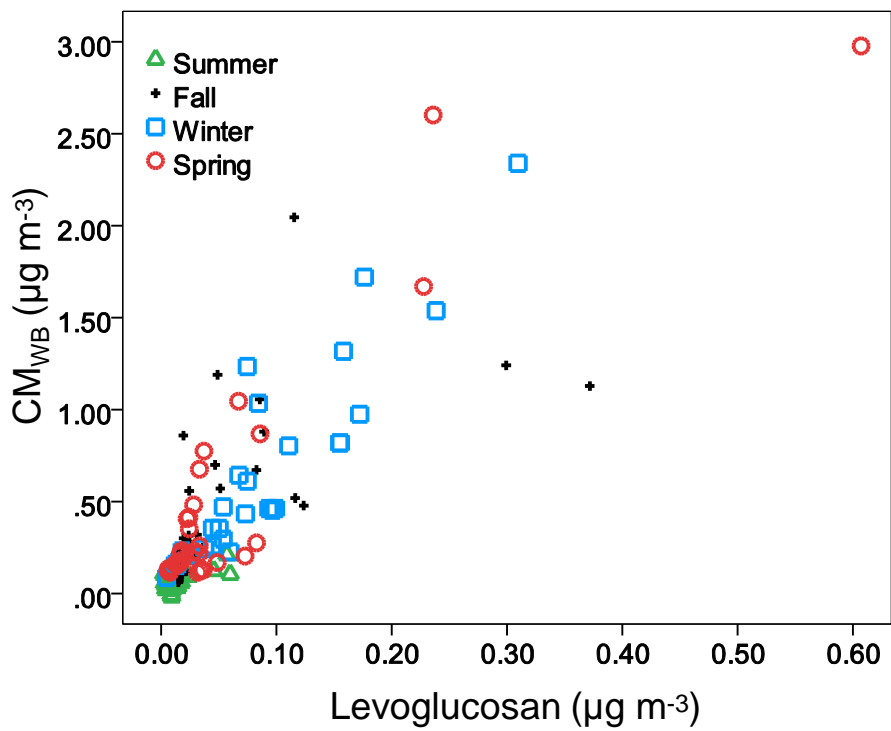
Figure 5: Comparison between CM$_{WB}$ and levoglucosan. R^2=0.70, N=122.
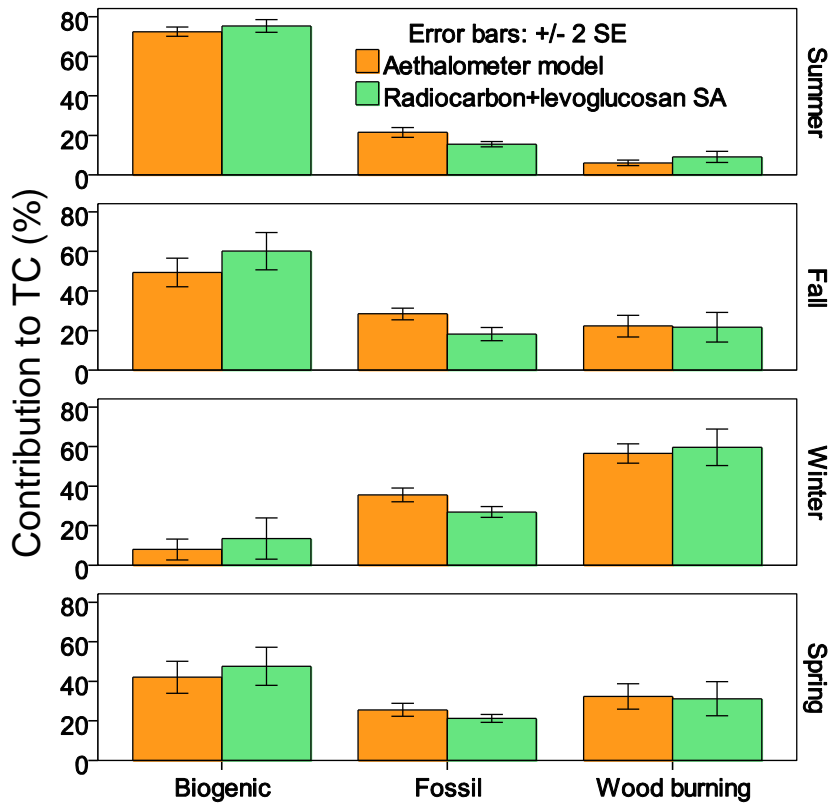
Figure 6: Seasonal comparison of source contribution to total carbon (TC) between the aethalometer model and radiocarbon + levoglucosan source apportionment (SA). Error bars display 2 times standard error of the mean (SE).